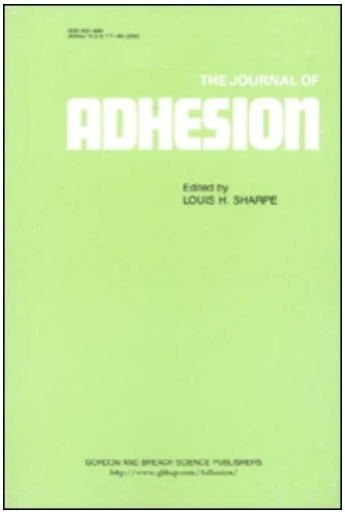

The Journal of Adhesion
Publication details, including instructions for authors and subscription information:
http://www.informaworld.com/smpp/title~content=t713453635

A Fracture Mechanics Approach to Failure in Fibrous Composites

Peter W. R. Beaumont[ab]
[a] Materials Department, School of Engineering and Applied Science University of California, Los Angeles, California, U.S.A. [b] Department of Engineering Materials, University of Cambridge, England

To cite this Article Beaumont, Peter W. R.(1974) 'A Fracture Mechanics Approach to Failure in Fibrous Composites', The Journal of Adhesion, 6: 1, 107 — 137
To link to this Article: DOI: 10.1080/00218467408072240
URL: http://dx.doi.org/10.1080/00218467408072240

J. Adhesion, 1974, Vol., 6 pp. 107–137

Printed in Northern Ireland

A Fracture Mechanics Approach to Failure in Fibrous Composites†

PETER W. R. BEAUMONT‡

Materials Department School of Engineering and Applied Science
University of California Los Angeles, California 90024 U.S.A.

(*Received March 21 1973*)

This paper presents a review of the fracture processes which occur in brittle thermosetting resins containing long strong fibers of carbon, boron and glass. Important material variables affecting the fracture behavior of the fibrous composite include fiber strength and strength of the fiber-matrix interface. Other parameters which must be considered include component geometry, environment, loading mode and nondestructive inspection capability. The effects of microstructural features including fiber volume fraction, together with a consideration of the fiber-resin interface are discussed in relation to the fracture stress and toughness of the composite material. The influence of the fiber-resin interface and environment on slow crack growth in carbon fiber-reinforced epoxy resin is also reviewed.

I INTRODUCTION

Extensive research efforts over the past decade in the field of materials science have concentrated on developing engineering materials of higher mechanical capability and structural reliability. The most dramatic improvements have been made where long strong fibers are introduced into conventional structural materials which normally would undergo plastic flow at low stresses. The fibers currently receiving the most interest are made of carbon, boron and glass. However, these fibers contain imperfections or flaws which may act as sites for the nucleation of microcracks followed by crack propagation through the fibrous composite. Whether brittle fracture will result from the earliest fiber break depends on (1) the form in which the

† Presented at the Symposium on "Interfacial Bonding and Fracture in Polymeric, Metallic and Ceramic Composites" at the Univ. of California at Los Angeles, Nov. 13–15, 1972. This Symposium was jointly sponsored by the Polymer Group of So. California Section, ACS and Materials Science Department, U.C.L.A.

‡ Now in Department of Engineering Materials, University of Cambridge, England.

stored elastic strain energy in the fiber is released and (2) the strength and toughness of the matrix and fiber-matrix interface. For example, if the energy is dissipated as kinetic energy there is the danger of catastrophic failure as one experiences in brittle ceramics and highly cross-linked polymers. The kinetic effects during extension of these flaws may be reduced, however, by expending the stored energy necessary to advance the crack to the next unbroken fiber in the form of "plastic" work at the crack tip. In general, the energy may be dissipated during crack propagation in fibrous composites by a multiplicity of microfracture events occurring at the crack tip including fiber fracture, G_f, matrix cracking, G_m, interfacial breakdown, G_d, fiber "relaxation", G_r, and fiber pull-out, G_p. The total work done per unit area of fracture, G, during crack progression may therefore be written as:

$$G = G_f + G_m + G_d + G_r + G_p \tag{1}$$

Typical values of G_f and G_m for ceramic fibers and thermosetting resins are unlikely to exceed $50\ \mathrm{Jm}^{-2}$ and $500\ \mathrm{Jm}^{-2}$, respectively, and the major contributions to the high fracture energies evaluated for these kinds of fibrous composites must come from these other possible sources.

For crack propagation through a single brittle fiber or monolithic brittle matrix, the fracture stress, σ_F, can be given by:

$$\sigma_F = \left(\frac{EG_c}{\pi a_c}\right)^{1/2} \quad (\sigma_F < \sigma \text{ yield}) \tag{2}$$

E is Young's modulus, G_c is the critical release rate of stored elastic strain energy per unit fracture area and a_c is the critical flaw size at fast (unstable) fracture. The major energy contributions which may be included in G_c *for a fibrous composite* are given in Eq. (1). Whether all or only some of these terms are included in G_c will depend on the mechanisms controlling crack initiation.

Although the conventional Charpy impact test can be used to measure G and allow simple comparisons of toughness to be made between different composite systems, it does not provide any useful information which may be directly applied to fracture safe design of fibrous materials. A more significant and useful parameter would be the stress intensity factor, K, used in classical linear elastic fracture mechanics analysis:

$$K = \sigma\sqrt{\pi a}\, f(g) \tag{3}$$

where σ is the applied stress, a is the flaw size and $f(g)$ is a geometric factor of the order of unity and dependent on flaw size and size of component. Under a certain stress and environmental condition, the flaw may slowly grow until it reaches a critical size, a_c, at which point the fracture stress of

the damaged material is given by:

$$\sigma_F = \frac{K_c}{\sqrt{\pi a_c}\, f(g)} \tag{4}$$

The relationship between critical stress intensity factor, K_c, and G_c is simply:

$$K_c = (EG_c)^{1/2} \quad \text{(plane stress)} \tag{5}$$

The critical flaw size, a_c, may be obtained by re-arranging Eq. (4):

$$a_c = \frac{1}{\pi}\left[\left(\frac{K_c}{\sigma}\right)\frac{1}{f(g)}\right]^2 \tag{6}$$

However, if the size of crack in a fibrous composite is substantially larger than the microstructural features, e.g., fiber diameter or interfiber spacing, the question arises whether these same concepts may be used to predict the fracture stress of a heterogeneous, anisotropic solid where fracture invariably occurs with crack branching, subsidiary cracking in the matrix and shear failure at the fiber-matrix interface close to the crack tip.

As an approximation, the fibrous composite may be considered an homogeneous, orthotropic solid. The Irwin-Westergaard expressions[1] describing the stress distribution adjacent to the crack tip will therefore be modified by functions containing the elastic constants of the material. The equations for stress equilibrium and strain compatibility at the crack front are not significantly affected by non-isotropy and the expressions for K in terms of stress and crack size will remain essentially the same. For crack propagation in a principle stress direction on a plane of elastic symmetry (Figure 1), the relationship between K_c and G_c is given by:[2]

$$K_c^2 = \left\{\left(\frac{a_{22}a_{11}}{2}\right)^{1/2}\left[\left(\frac{a_{22}}{a_{11}}\right)^{1/2} + \left(\frac{a_{66} + 2a_{12}}{2a_{11}}\right)\right]^{1/2}\right\}^{-1} G_c \tag{7}$$

The orthotropic compliance values, a_{11}, a_{22}, etc., may be determined either experimentally or derived theoretically from the elastic constants of the fiber and matrix.[3] A comparison between Eqs. (5) and (7) indicates E has been replaced with an "effective modulus" parameter, E', for the orthotropic solid, where

$$E' = \left\{\left(\frac{a_{22}a_{11}}{2}\right)^{1/2}\left[\left(\frac{a_{22}}{a_{11}}\right)^{1/2} + \left(\frac{a_{66} + 2a_{12}}{2a_{11}}\right)\right]^{1/2}\right\}^{-1} \tag{8}$$

The calculation of G in terms of K is therefore essentially identical for both orthotropic and isotropic cases where E is the elastic modulus of an isotropic material and E' is a function of the elastic constants of an orthotropic solid. G can also be expressed in terms of a change of specimen compliance with

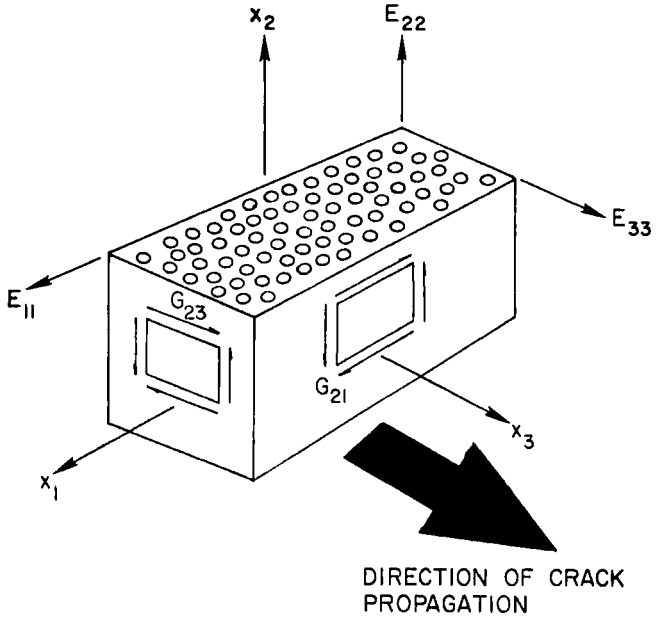

$$G_{IC} = K_{IC}^2 \left(\frac{a_{11}a_{22}}{2}\right)^{1/2} \left[\left(\frac{a_{22}}{a_{11}}\right)^{1/2} + \frac{2a_{12}+a_{66}}{2a_{11}}\right]^{1/2}$$

FIGURE 1 The relationship between principle stress direction, fiber orientation and direction of crack propagation.

increasing crack length where

$$G_I = \frac{1}{2}\frac{P^2}{B}\left[\frac{d(1/s)}{da}\right]_a \tag{9}$$

P is load, s is stiffness and B is thickness of specimen. From Eqs. (7), (8) and (9) the relationship between K and change of specimen compliance of an orthotropic solid with increasing crack size is simply:

$$K_I = P\left[\left(\frac{E'}{2B}\right)\frac{d(1/s)}{da}\right]_a^{1/2} \tag{10}$$

II OBJECT

The formation and propagation of microcracks parallel to fibers is relatively harmless in terms of reducing the load carrying capability of a unidirectional composite. This paper will therefore confine itself to evaluating the effect of cracks progressing perpendicular to fibers and direction of applied stress in

terms of the static and dynamic properties of the composite. Primarily, we will see how far the ideas of linear elastic fracture mechanics analysis can provide a rational approach to fracture safe design of fibrous materials. Secondly, we will attempt to evaluate the particular microfracture processes which control crack initiation and crack propagation. The microstructural aspects of crack propagation is discussed, together with the role of the fiber-matrix interface in influencing failure processes. Special attention is given to aligned carbon fiber-reinforced epoxy resin and polyester resin composites but wherever possible comparisons are made between these materials and polymer composites containing fibers of boron or glass (Table I).

TABLE I
The fibrous composites

Fiber	Matrix	Fiber volume fraction (V_f)	Fiber properties		
			Diameter (m)	Tensile strength (GNm^{-2})	Young's Modulus (GNm^{-2})
RAE type I Carbon fiber Surface untreated	Epoxy 828/MNA/ BDMA	0.4	8×10^{-6}	1.58	360
RAE type I Carbon fiber Surface treated	Epoxy 828/MNA/ BDMA	0.4 0.45 0.52 0.60	8×10^{-6}	1.58	360
Whittaker-Morgan Type II Carbon fiber Surface treated	Proprietary Epoxy resin	0.64	8×10^{-6}	2.41	240
Boron fiber	Union Carbide ERLA 2256-0820	0.66	1×10^{-4}	3.1	360
S-glass	Proprietary Epoxy resin	0.76	1×10^{-5}	3.44	85.5
E-glass[a]	Proprietary Polyester Resin	0.15	1×10^{-5}	2.10	72.0

[a] Random orientation of *E*-glass fibers only.

III EXPERIMENTAL

3.1 Measurement of fracture stress

The fracture stress of a fibrous composite containing a sharp notch or crack can be evaluated from tensile or flexural experiments. The problem lies mainly in producing a sharp crack since splitting is likely to occur parallel to fibers at the crack tip in a tensile experiment on thin sheet material. The alternative is to introduce side grooves in the plane of the crack normal to

fibers, thereby reducing the critical load for unstable fracture. Center and edge notches can be introduced with a jeweler's saw or fine slitting wheel and the notch tip sharpened with a scalpel blade. The notch size will therefore be very large compared to the microstructural features of the composite material. Any attempt to produce a real crack by tensile load cycling will simply result in fatigue failure at the fiber-matrix interface and so *reduce* the concentration of stress at the root of the notch. If the initial fracture event occurs from a sharp notch rather than at a single crack tip, the fracture stress must be considered a maximum value. The specimen designs which have been used are illustrated schematically in Figure 2, together with typical load/deflexion curves obtained for some carbon, boron and glass fiber composites.

3.2 Measurement of fracture toughness

Using Eq. (3) and a knowledge of σ_F and a_c for a particular fibrous composite can lead to the fracture toughness, K_{Ic} value. The geometrical factor included in Eq. (3) for the particular specimen design can be obtained from the ASTM publication on Fracture Toughness Testing.[4] An exact solution of K using Eq. (3) is prevented by the anisotropy of the composite system, but for the specimen geometry and composite materials described any error will be within the normal experimental scatter of fracture stress.

K_{Ic} is a useful parameter for predicting conditions for fracture safe design. Alternately, G_{Ic} can be calculated using Eq. (7) (assuming plane strain conditions exist) and related to the energy absorbing fracture processes which occur in a microfracture process zone at the crack front. An evaluation of G should provide an indication of the important microstructural features affecting crack initiation and crack progression in the fibrous composites. Similarly, the compliance analysis method may be used to estimate G_{Ic} (Eq. 9). This empirical approach can be compared to the analytical method of linear elastic fracture mechanics.

3.3 Work of fracture

Crack propagation in brittle fiber composites may be "controlled" by designing the flexural specimens in such a way that the maximum stored elastic strain energy at fracture is small compared with the surface energy required to break the specimen. A rectangular beam specimen containing a triangular cross section at its midpoint has been used in an attempt to achieve these conditions. The area under the load/deflexion curve may be equated to the work to completely fracture the specimen.[5] This will include the crack initiation energy and crack propagation energy. The specimen is essentially

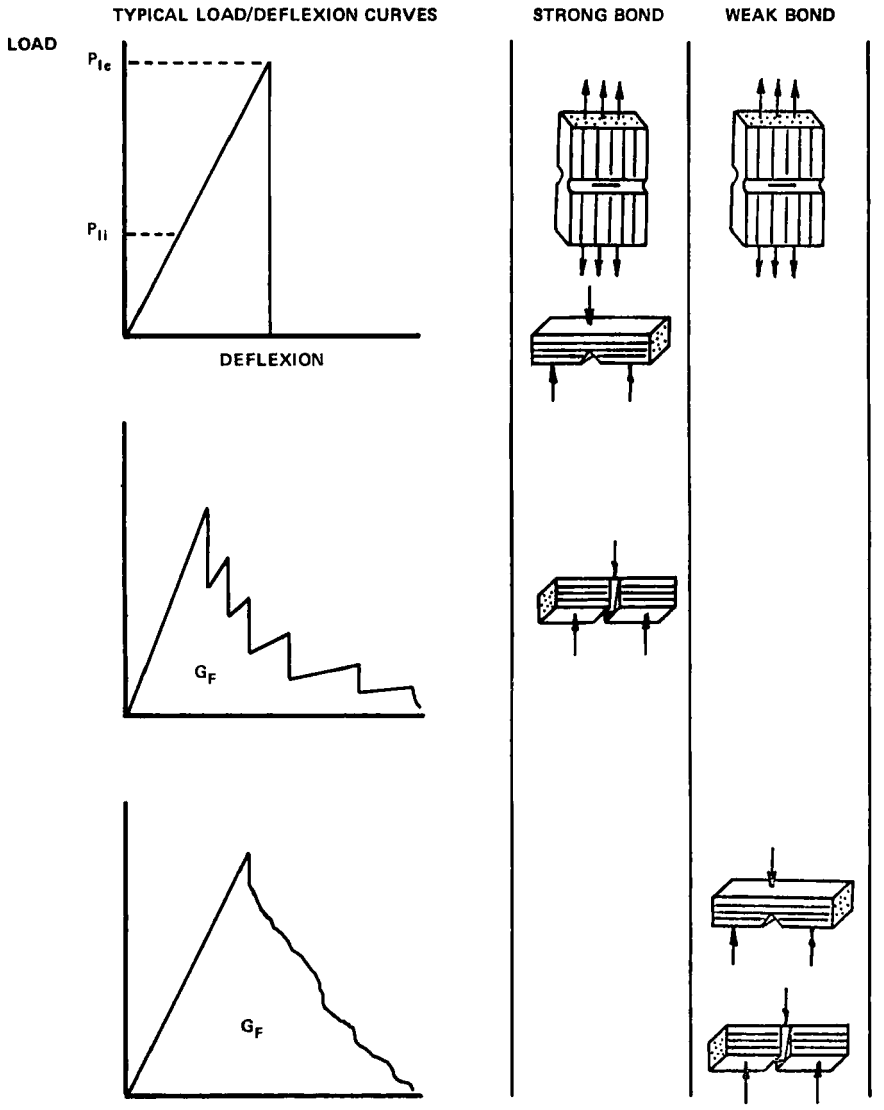

FIGURE 2 Specimen designs and typical load/deflexion curves for carbon, boron and glass fiber-reinforced thermosetting resin composites.

a "decreasing K" specimen where the thickness increases as the crack extends and ideally, work is continually required to propagate a moving crack. In brittle fibrous composites, however, fracture of the decreasing K specimen will occur in a "quasi-controlled" manner and the *work of fracture*, G_F,

will contain some kinetic energy and must then be considered a maximum value (Figure 2). (G_F is determined by integrating the load/deflexion curve and dividing by the fracture area). Providing the size of the microfracture process zone at the crack tip does not change significantly as the crack extends, one might expect values of G evaluated analytically and empirically to be similar.

3.4 Detection of microcrack growth at $K_I < K_{Ic}$

An acoustic emission technique has been used to determine the onset of damage in the fibrous composite at $K_I < K_{Ic}$. The critical threshold value of K at which the first occurence of microfracture is detected is called K_{Ii}. The value of K_{Ii} corresponds to a rapid increase in acoustic emission count rate ($\dot{N}$) recorded using a standard Dunegan Corporation apparatus. Acoustic emission is derived principally from the stored elastic strain energy in the fibers which is emitted when the fiber breaks.

IV RESULTS

4.1 Effect of crack size and specimen geometry on fracture toughness

Experimental values of K_{Ic} and K_{Ii} as a function of crack size for a surface treated, *high modulus* carbon fiber-epoxy resin composite (high bond strength) are shown in Figure 3a. It is apparent that K_{Ic} and K_{Ii} are independent of crack length, as one would expect if linear elastic fracture mechanics analysis is applicable to these materials and testing conditions. Superimposed in the figure is the value of K_{Ic} evaluated for a 40 percent (by vol.) carbon fiber composite by inserting an experimental value of G_F equal to 8 kJm^{-2} and theoretical E' value of 37 GNm^{-2} into Eq. (7), which may be re-written as

$$K_{Ic} = (E'G_F)^{1/2} \tag{11}$$

The value of K_{Ic} is shown as a broken line independent of crack length. These two quite distinct approaches for determining K_{Ic} are in good agreement, particularly in view of the assumptions made earlier. A 50 percent probability of failure occurs at K_{Ic} equal to 15.2 $MNm^{-3/2}$ which compares favorably with the value of 17 $MNm^{-3/2}$ calculated using Eq. (11). The compliance analysis produces results which fall between these two values. Similar trends are also observed for a higher fiber volume fraction composite (Figure 3b) and a surface treated, *high strength* carbon fiber-epoxy resin composite. Typical experimental values of K_{Ic} and K_{Ii} for a boron fiber and high strength carbon fiber composite are shown in Figure 4.

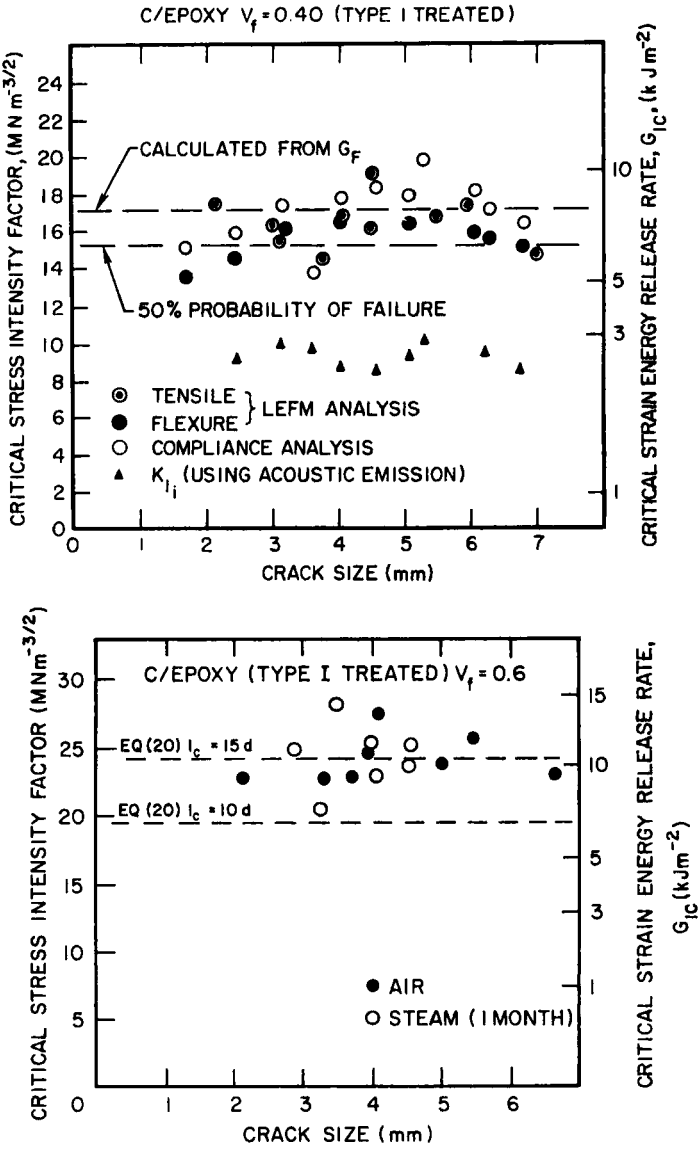

FIGURE 3 Some experimental values of critical stress intensity factor as a function of crack size for (a) surface treated type I 40 percent (by vol.) carbon fiber-epoxy resin and (b) a similar composite containing 60 percent (by vol.).

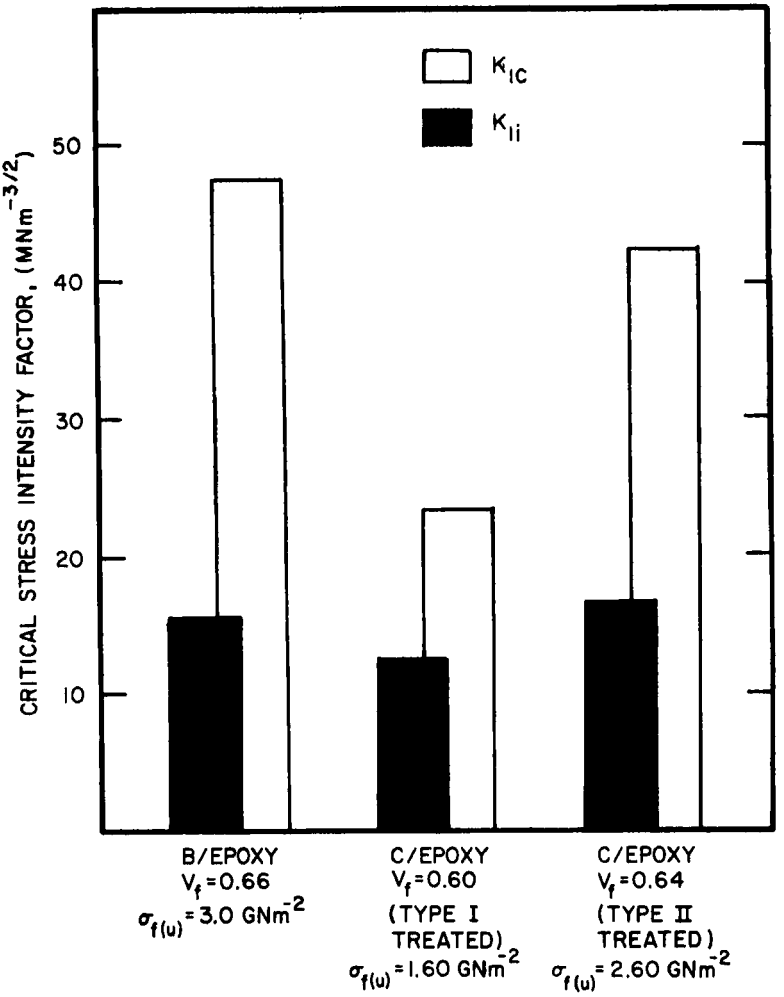

FIGURE 4 Some typical values of critical stress intensity factor for carbon fiber and boron fiber composites.

The tensile experiments were carried out using plates 12.5 mm wide and a minimum thickness between the center grooves of 1 mm. Similar tensile tests have been carried out[6] on 57 mm wide plates (a/w held constant at 0.4) and an average K_{Ic} value of 18 $MNm^{-3/2}$ measured for a 40 percent (by vol.) high modulus carbon fiber composite. This value is within the experimental scatter observed using narrow specimens. In contrast, experiments carried out using surface untreated carbon fiber and *S*-glass fiber-epoxy resin composites of *low bond strength*, showed almost complete *notch insensitivity*

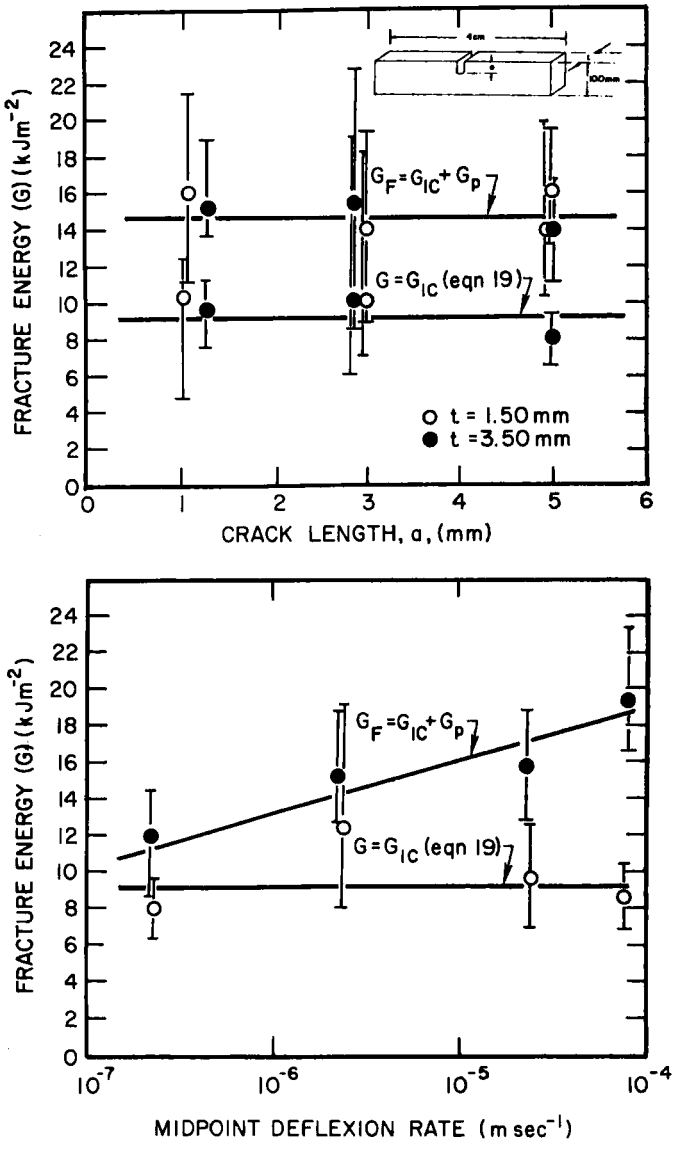

FIGURE 5 Some experimental values of toughness (G_{Ic}) and work of fracture (G_F) as a function of crack size for a random *E*-glass fiber-polyester resin composite ($V_f = 0.15$).[8]

at all crack lengths rendering linear elastic fracture mechanics analysis invalid.[7]

Figure 5 shows experimental values of G as a function of crack size for a random E-glass fiber-polyester resin composite. The linear elastic fracture mechanics and work of fracture experiments were carried out using notched beam specimens loaded in three-point bending. Unlike the results obtained on carbon fiber composites, the two experimental approaches produced two quite distinct critical values of G both independent of crack size. It appears that the energy to initiate a crack (G_{Ic}) is less than the energy required for crack propagation (G_F) and additional work is therefore required for crack progression. The crack initiation energy is also independent of loading rate whilst the energy of crack propagation is a function of loading rate. A possible interpretation of G_{Ic} and G_F in terms of various fracture processes is presented in Section 6.

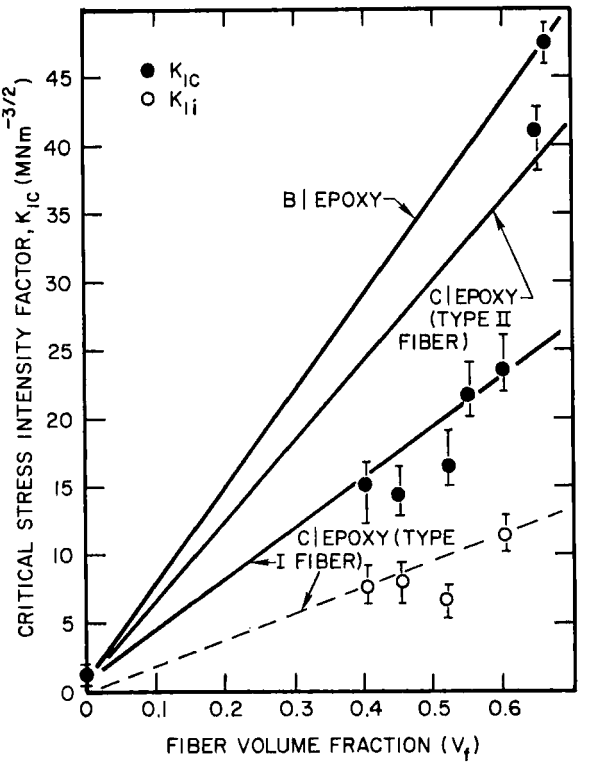

FIGURE 6 Some experimental and theoretical values of fracture toughness (K_{Ic}) for carbon fiber and boron fiber-reinforced epoxy resin composites as a function of fiber olume fraction.[9]

4.2 Effect of fiber volume fraction on KI_c

An increase in fiber volume fraction from 40 percent to 60 percent (by vol.) for surface treated, high modulus carbon fiber composites has resulted in an increase in K_{Ic} value from about 15 $MNm^{-3/2}$ to 23 $MNm^{-3/2}$ (Figure 6). Experimental results for a boron fiber and high strength carbon fiber–epoxy resin composite (V_f constant) have been included in the figure also. The solid lines showing proportionality between K_{Ic} and V_f are plots of Eq. (11) as a function of V_f for different experimental values of G_f and theoretical values of E'. Reasonable agreement is found between the analytical and empirical approaches to the fracture toughness of these strongly-bonded fibrous composites.

V FRACTURE SAFE DESIGN

The fracture stress of a strongly-bonded fibrous composite investigated can be reasonably well predicted using the equation:

$$\sigma_F = \frac{K_{Ic}}{\sqrt{\pi a_c}} \tag{12}$$

where the crack size, a_c, is significantly less than the size of component but much greater than any microstructural feature. This is a low fracture stress criterion of a brittle solid containing a sharp crack and is extremely useful for predicting fracture safe design with brittle materials. A knowledge of K_{Ic} and the maximum flaw size in the material which may be detected using an NDT technique, will allow determination of the maximum stress, σ_F. It is important to realize that improvements in NDT may raise the highest stress which can safely be applied in service by reducing the size of the detectable flaw.

In unidirectional fiber composites, E' is approximately proportional to V_f[9] and we will see later that a simple linear relationship exists also between G and V_f (Section 6). Equation (11) can therefore, be re-written as:

$$K_{Ic} = kV_f \tag{13}$$

or,

$$\sigma_F = k'V_f \tag{14}$$

where k and k' are constants for a particular fiber composite. This has been verified experimentally (Figure 6) and therefore we are now in a position to compare these fibrous materials for structural applications.

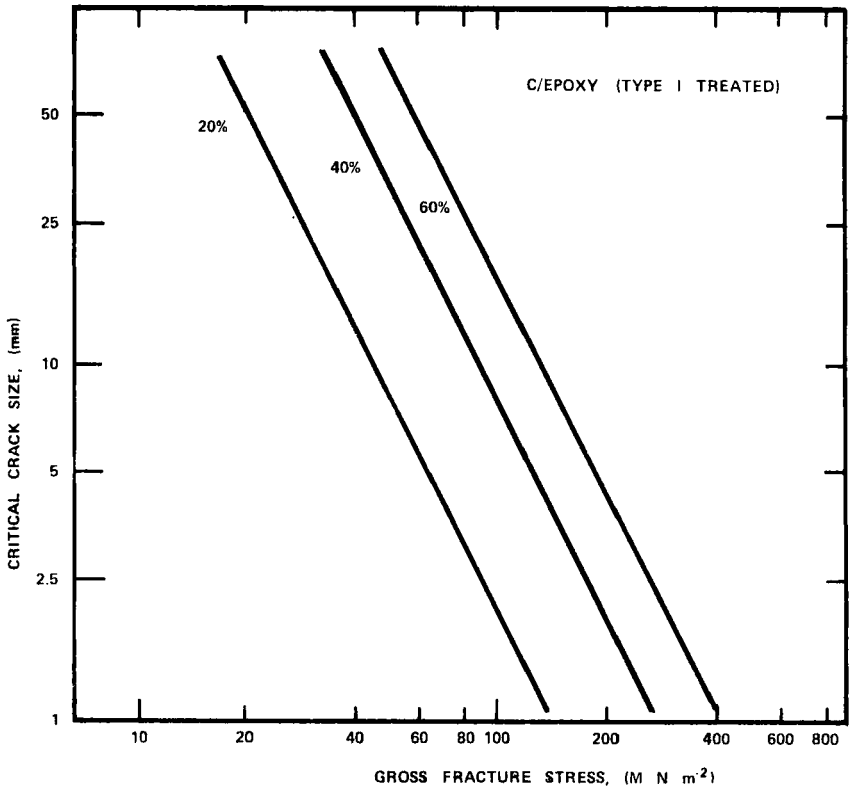

FIGURE 7 The fracture stress of some surface treated type I carbon fiber-epoxy resin composites as a function of crack size.

Figure 7 shows the fracture stress of high modulus carbon fiber-epoxy resin composites over a range of V_f evaluated using Eq. (12). At a particular working stress level, σ_w (where $\sigma_w = \sigma_F/N$ and N is a safety factor > 1), the critical flaw size may be increased by an order of magnitude simply by incorporating three times as much fiber into the matrix. Similarly, the critical flaw size may be increased about three fold by selecting boron fibers rather than high modulus carbon fibers (V_f constant) (Figure 8). Alternately, for a given flaw size, the fracture stress, σ_F (and hence σ_w), may be raised by a factor of 2 by choosing boron fibers rather than high modulus carbon fibers (V_f constant). At a particular working stress, σ_w, less boron fibers would be needed but the question of economics as well as mechanical performance must be considered. It is predicted that carbon fibers will become significantly cheaper than boron fibers and this may therefore be an overriding factor in selecting carbon fibers from a composite fracture stress

versus cost standpoint. Improvements in NDT capability to reduce the critical flaw size should result in a decrease in price of composite since σ_F depends on V_f as well as a_c (Eq. 14). There would be certain economic gains in using low values of V_f providing a_c falls within inspection limits. Fracture safe design also requires detection of the initial flaw of size $a_i < a_c$ before crack growth occurs under stable conditions, in order to predict the life expectancy of the component (see Section 7).

An important material parameter from a designer's viewpoint is the specific fracture stress (σ_F/ρ). The specific fracture stress of a few structural materials including these fibrous composites is plotted in Figure 9 as a function of flaw size. The aluminum alloy has the highest fracture stress: weight ratio for flaw sizes less than 4 mm. Of the crack sensitive fibrous materials, high strength carbon fiber composites are superior and the high modulus carbon fibers and boron fibers produce composites having a similar specific fracture stress. For example, at a particular σ_w, the critical

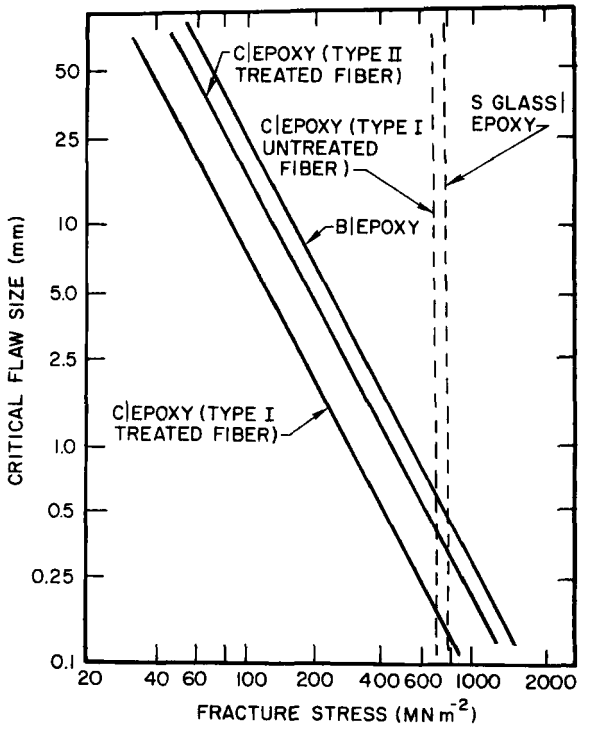

FIGURE 8 The fracture stress of carbon, boron and glass fiber-epoxy resin composites as a function of crack size ($V_f = 0.40$).

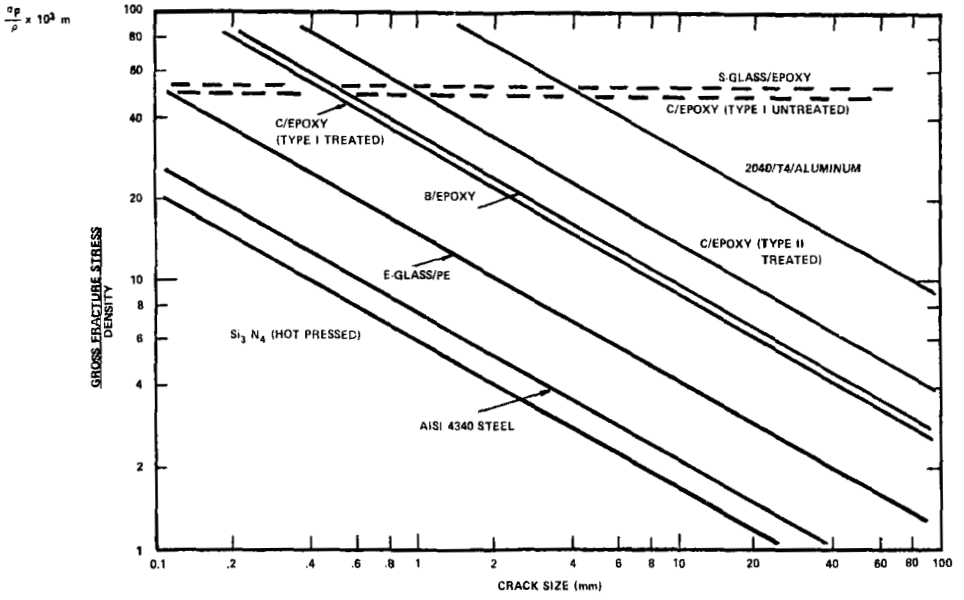

FIGURE 9 The specific fracture stress of some engineering materials as a function of crack size. (The composite materials contain 40 percent (by vol.) of fiber.)

crack size of a 40 percent (by vol.) high strength carbon fiber composite is more than an order of magnitude greater than for a high strength steel. The *notch-insensitive, weakly-bonded fibrous composites* containing carbon and *S*-glass fibers have been included in the figure for comparative purposes only. Increasing the fiber volume fraction will shift the curves of the notch-sensitive fibrous materials to the right and the notch-insensitive composites upwards. Unfortunately, the low bond strength composites exhibit poor transverse strength and torsional properties.

VI MICROSTRUCTURAL ASPECTS OF CRACK PROGRESSION

Crack initiation in brittle fibrous composites occurs by the breakage of fibers at flaws close to the crack tip and cracking in the matrix between broken fibers (Figure 10). The process of crack growth involves displacement of the fracture surfaces at the crack tip and pulling out of broken fibers bridging the matrix crack behind the tip. Consequently, fractographs of composite materials containing brittle fibers show the characteristic fibrous

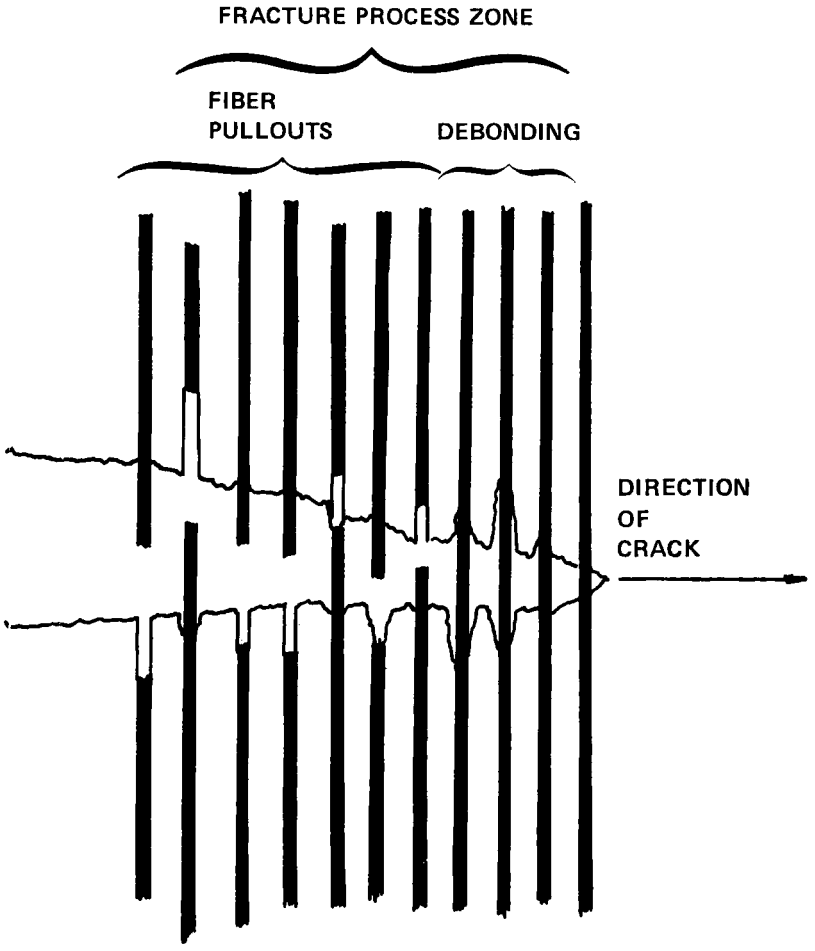

FIGURE 10 A schematic representation of some possible microfracture processes occurring at the tip of a crack in a brittle fibrous composite.

appearance. Assuming that reloading of the fiber occurs after fiber fracture, then the maximum length of protruding fiber out of the surface of the matrix will be $l_c/2$ where l_c is defined by:[10]

$$l_c = \frac{\sigma_{f(u)} d}{2\tau_i} \tag{15}$$

l_c is called the critical fiber length, $\sigma_{f(u)}$ is the fiber strength, d the fiber diameter and τ_i the interfacial shear stress.

The extension of a crack may be considered a two stage process: (1) crack initiation and (2) crack propagation. If the length of fiber pulled out of the

resin matrix is small compared to the size of fracture process zone, then the work done in opening the crack surfaces at the tip will include the term G_p, as well as G_f, G_m, G_r, and G_d, and the crack initiation energy will be similar to crack propagation energy. Conversely, if the fiber pull-out length is similar to the size of fracture process zone, then crack initiation energy may simply be the sum of the terms G_f, G_m, G_r and G_d and the work to pull broken fibers out of the matrix G_p, will contribute to the energy of crack propagation only.

6.1 Energy for crack progression, G

When a fiber close to the crack tip snaps, the amount of energy released is simply

$$\Delta E_g = \frac{\pi \, \mathrm{d}^2 \sigma_{f(u)}^2 l_c}{12 E_f} \tag{16}$$

where E_f is the fiber modulus and l_c is the length of fiber over which relaxation has occurred. For a fiber composite having a fiber volume fraction V_f:

$$G_r = \frac{4 \Delta E_g V_f}{\pi \, \mathrm{d}^2} \tag{17}$$

$$= \frac{V_f \sigma_{f(u)}^2 2 l_c}{3 E_f} \tag{18}$$

where G_r is the "fiber relaxation energy" per unit fracture area of composite.[11]

The average length of protruding boron fiber from the fracture surface of the composite is about 1.5×10^{-3} m. Inserting the appropriate values of V_f, $\sigma_{f(u)}$, E_f and $l_c = 6 \times 10^{-3}$ m into Eq. (18) gives a value of G_r equal to 28 $\mathrm{kJm^{-2}}$. This is in good agreement with experimental values of G_{Ic} and G_F of approximately 35 $\mathrm{kJm^{-2}}$. If debonding occurs over a portion of the fiber length, Y, such that τ_i tends to zero, then[12]

$$G_d = \frac{V_f \sigma_{f(u)}^2 Y}{2 E_f} \tag{19}$$

The distance over which debonding of the S-glass fiber occurred is estimated to be 1×10^{-3} m from pull-out measurements. Using Eq. (19), G_d is calculated to be 210 $\mathrm{kJm^{-2}}$ which compares favorably with the experimental G_F value of 242 $\mathrm{kJm^{-2}}$.

An analysis originally derived to account for the energy dissipated during extraction of discontinuous fibers[13] of length l_c may be used to approximate the pull-out energy of a continuous fiber composite with a distribution of

fiber strengths by assuming that the mean fiber pull-out length is equal to $l_c/4$, and therefore

$$G_p = \frac{V_f \sigma_{f(u)} l_c}{12} \tag{20}$$

$$= \frac{V_f \tau_i' l_c^2}{6\,\mathrm{d}} \tag{21}$$

Using scanning electron microscopy, the average length of surface treated type I carbon fiber protruding out of the matrix is estimated between 3 and 4 diameters. Figure 11 shows three theoretical plots of Eq. (20) where values of l_c = 10 d, 15 d and 20 d, have been inserted, respectively together with

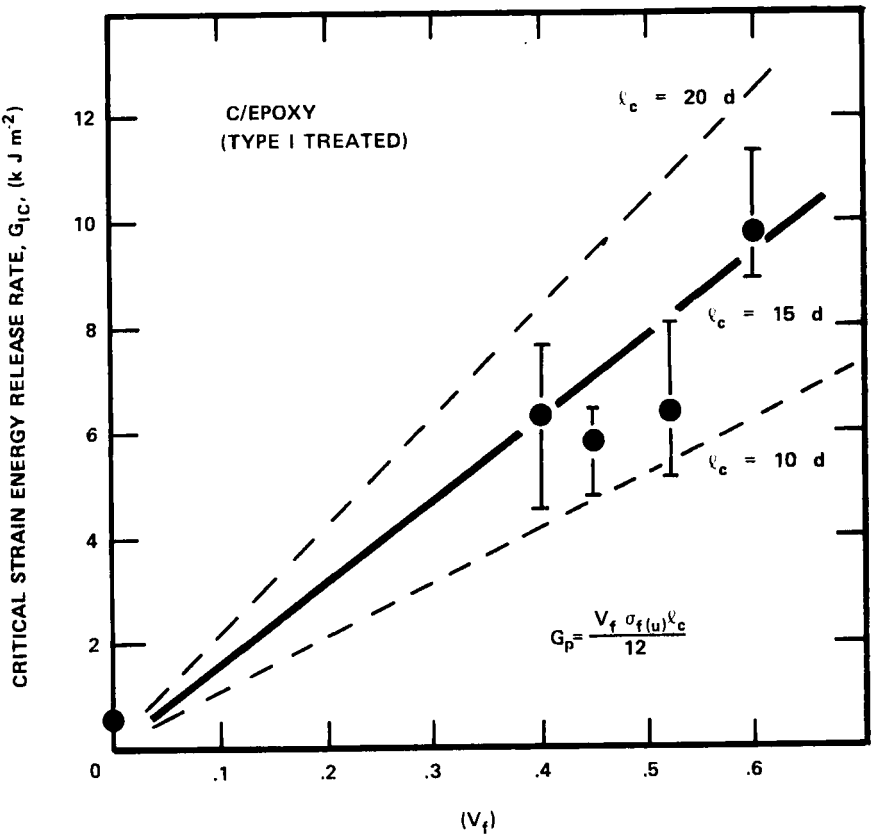

FIGURE 11 Some experimental and theoretical values of toughness of surface treated type I carbon fiber-epoxy resin as a function of fiber volume fraction using the pull-out model.

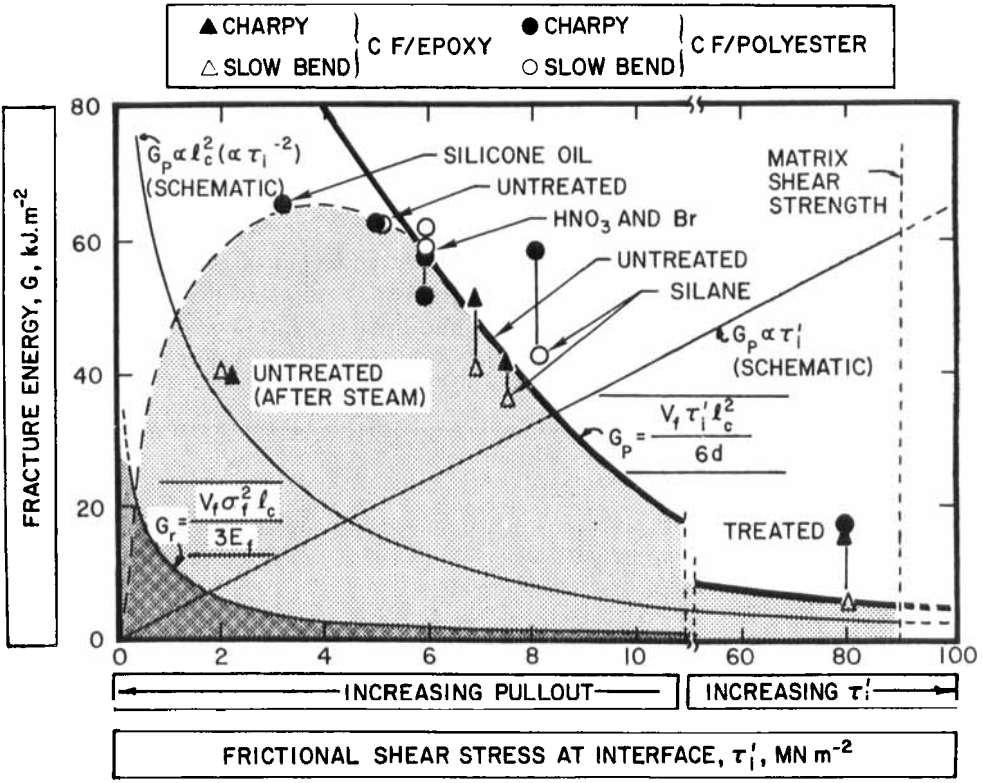

FIGURE 12 Some experimental and theoretical values of toughness of type I carbon fiber-reinforced thermosetting resin composites as a function of bond strength.[14]

values of G_{Ic} calculated from the measured values of K_{Ic}. Good agreement is found between the experimental values of G_{Ic} and theoretical G_p values where l_c is between 10 and 15 d, equivalent to the value of l_c estimated from fiber pull-out measurements. Similarly, where τ_i' has been significantly affected by various fiber surface treatments and the resulting average fiber pull-out length has varied between about 3 and 30 fiber diameters depending on bond strength, good agreement is found between the work of fracture, G_F values and the theoretical fiber pull-out energy, G_p (Eq. 21) above a critical value of frictional interfacial shear stress ($\tau_i' \approx 6\ \mathrm{MNm^{-2}}$) (Figure 12). Exposing the surface untreated carbon fiber composite to steam resulted in a decrease in τ_i and a corresponding increase in l_c by a factor of 2, to approximately 200 d estimated from fiber pull-out measurements. The fiber pull-out length depends on the value of τ_i and the work to pull the fiber out of the matrix is determined by the frictional interfacial shear stress τ_i'. By

substituting $G_F = 40\ \text{kJm}^{-2}$ and $l_c = 200\ \text{d}$ into Eq. (21), τ_i' is calculated to be $2\ \text{MNm}^{-2}$ which is a factor of 3 less than τ_i' estimated in dry conditions. The effect of moisture has been to reduce the compressive forces exerted by the matrix over the surfaces of fibers by resin swelling and to provide a lubricant at the fiber-matrix interface. Exposure of surface treated carbon fiber composites to steam had little or no significant effect on K_{Ic}, (Figure 3b) or τ_i' and G_F.

During loading of the random *E*-glass fiber composites severe crazing occurred at the crack tip at about $K_I = 0.5\ K_{Ic}$. At the instant of fast fracture, the diameter of this fracture process zone is about 4 mm which may be considered as the distance over which fiber debonding has taken place.[8] Inserting, therefore $Y = 4$ mm, $\sigma_{f(u)} = 2.1\ \text{GNm}^{-2}$, $E_f = 72\ \text{GNm}^{-2}$ and $V_f = 0.075$, (we will assume that only one-half of the random fibers ($V_f = 0.15$) will actually pull-out of the resin), into Eq. (19) results in a theoretical value of G_d close to $9\ \text{kJm}^{-2}$. This agrees well with the experimental values of G_{Ic} (Figure 5a). The difference between the experimental values of G_F and G_{Ic} is equal to $6\ \text{kJm}^{-2}$ and may be due to the additional work required to extract the broken glass fibers out of the resin during crack progression, G_p. Using Eq. (21), we find that τ_i' lies between zero and $0.5\ \text{MNm}^{-2}$ depending on the rate of loading or rate of fiber extraction (Figure 5b). This is about an order of magnitude less than the value of τ_i measured prior to fiber debonding.[15]

The increase in G_F for the random *E*-glass fiber composite with increasing strain rate, (G_{Ic} remaining unaffected) shown in Figure 5b indicates that the crack propagation energy becomes greater the higher the strain rate. This may be related to crack velocity and the viscoelastic nature of the resin matrix and hence a time dependence of the parameter, τ_i'. By a similar approach, the small increase in G_F for surface untreated fiber composites over 7 decades of strain rate merely reflects an increase in τ_i' by about 5 percent[16] but the effect is more marked for the higher bond strength material (Figure 13). Estimations of the various energy contributions to the toughness of the fiber composites are presented in Table II.

The major contribution to the fracture initiation energy, G_{Ic}, of the boron and glass fiber composites is from the stored elastic strain energy in the stressed fibers. Increasing the crack velocity in the *E*-glass fiber composite results in an increase in crack propagation energy due to the time dependence of τ_i' on the pull-out energy, G_p. For carbon fiber composites, the fiber debonding and relaxation energies are small. Additional work to extract the fibers over a small distance at the crack tip against the interfacial frictional forces accounts primarily for the values of G_{Ic} and G_p. The crack propagation energy of a carbon fiber composite is therefore approximately equal to the crack initiation energy.

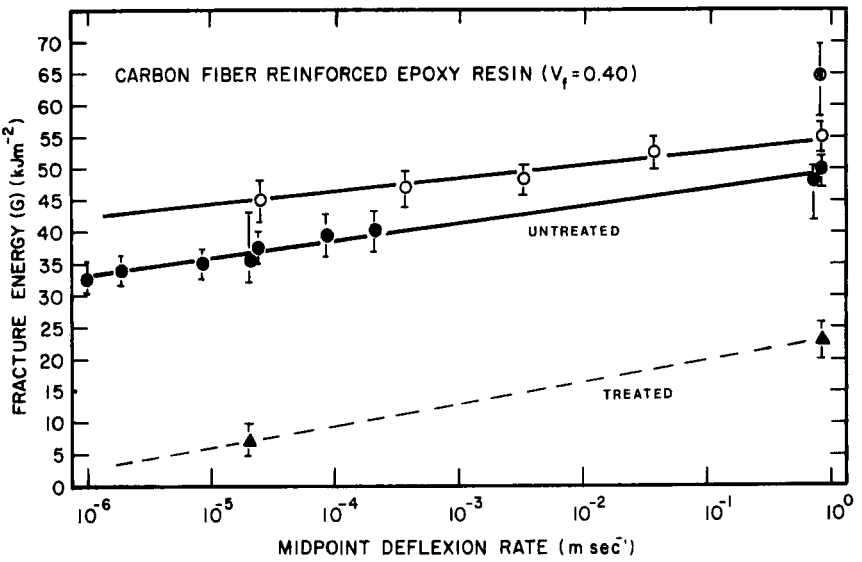

FIGURE 13 Some experimental values of fracture energy (G) of two carbon fiber-epoxy resin composites as a function of loading rate. (○ 4-point bending; ● 3-point bending;[16] ▲ 4-point bending[6]).

TABLE II
Estimation of energy to propagate a crack

Material	K_{Ic} (MNm$^{-3/2}$)	G_{Ic} (kJm^{-2})	G_F (kJm^{-2})	$lc/4$ (m)	$G_r = \frac{V_f\sigma_f^2 l_c}{3E_f}$ (kJm^{-2})	$G_d = \frac{V_f\sigma_f^2 Y}{2E_f}$ (kJm^{-2})	$G_p = \frac{V_f\sigma_f l_c}{12}$ (kJm^{-2})
40% CFRP (type I untreated)	—	—	37.4	2.4×10^{-4}	0.94	1.4	52.0
40% CFRP (type I treated)	15.2	6.4	8.0	2×10^{-5}	0.08	0.12	5.0
64% CFRP (type II treated)	40.0	36.0	29.2	5×10^{-5}	1.02	1.54	25.8
66% B/Epoxy	47.0	34.6	35.0	1.5×10^{-3}	28.0	42.0	1400
76% S glass/ Epoxy	—	—	242	1×10^{-3}	140.0	210	872
828/BDMA/MNA Epoxy resin	1.54	0.7	1.0	—	—	—	—
Polyester Resin	1.20	0.44	0.44	—	—	—	—

6.2 Acoustic emission and fracture energy

Localized microcrack growth has been detected in carbon and boron fiber composites at $K_{Ii} < K_{Ic}$ using an acoustic emission technique. If we assume that the rapid increase in acoustic emission count rate, $\dot{N}$, is due to the fracture of fibers close to the crack tip, then the energy released in breaking a single fiber is given by Eq. (16) and the toughness, G_{Ic} of the composite is simply calculated knowing the volume fraction of fibers. Harris *et al.*[17] have proposed that the initial voltage output from the transducer, V_o, is proportional to the square root of the energy released during a particular deformation process:

$$V_o = \psi(\Delta E_g)^{1/2} \tag{22}$$

They have shown that the number of "counts", N_T, associated with the damped sinusoidal acoustic signals is given by:

$$N_T = \frac{f}{\beta} \ln\left(\frac{V_o}{V_t}\right) \tag{23}$$

where f is the linear frequency, β is a damping constant and V_t is a threshold voltage. Combining Eqs. (22) and (23) and solving for N_T:

$$N_T = \frac{f}{2\beta} \ln\left[\frac{\psi^2(\Delta E_g)}{V_t^2}\right] \tag{24}$$

If a constant number of fiber breaks occur within the microfracture process zone as the crack extends, then the number of counts per unit fracture area is given by:

$$\frac{dN_T}{dA} \alpha \ln(\Delta E_g) \tag{25}$$

or since $\Delta E_g \equiv (G/\lambda)$, then

$$\frac{dN_T}{dA} \alpha \ln(G) \tag{26}$$

This is illustrated in Figure 14 for a boron fiber-reinforced epoxy resin composite, where G and dN_T/da both increased as the crack extended in the "decreasing K" specimen. Acoustic emission testing, therefore, provides a useful NDT technique for estimating the amount of damage in a composite due to shock or impact loading.

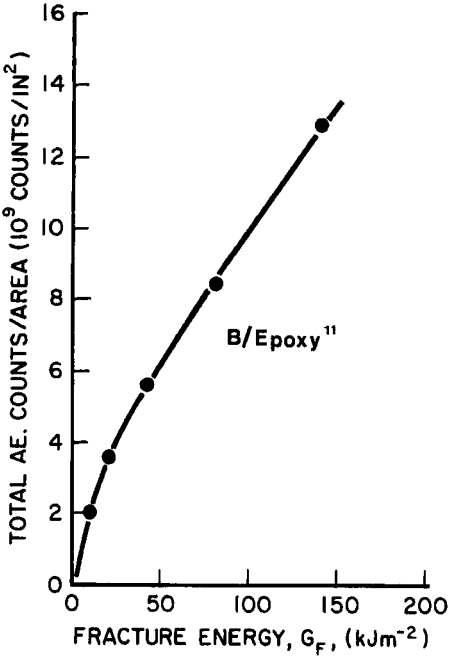

FIGURE 14 Variation of total number of acoustic emission counts/area with G for the decreasing K specimen.[11]

VII TIME-DEPENDENT BEHAVIOR

If linear elastic fracture mechanics analysis is applicable to certain fibrous composites, then a knowledge of the crack growth rate at a particular working stress can be applied to predicting the lifetime of the material or the time required for a crack of size a_i to propagate to a_c (Eq. 6). An analytical expression proposed to compute structural lifetime is:

$$\frac{da}{dN} = A(\Delta K)^n \tag{27}$$

$$= A(\Delta\sigma\sqrt{\pi a})^n \tag{28}$$

where ΔK is the stress intensity range in one cycle, N is the number of cycles and A and n are material and environmental constants. If the minimum applied stress in a single cycle is zero, then

$$\int_{a_i}^{a_c} \frac{da}{A(K)^n} = \int_{N=0}^{N=N_F} dN \tag{29}$$

Berg and Salama[18] have observed slow crack growth tranverse to aligned

carbon fibers in an epoxy resin matrix, where the fatigue crack is loaded under compressive forces. Figure 15 shows the initial crack growth rate as a function of K^2 plotted from their data. From this curve $n \approx 12$ and since $a_c = (K_{Ic}^2/\pi\sigma^2)$ we have that

$$N_F = \frac{1}{A'\sigma^2\pi}\left(\frac{1}{K_i^{10}} - \frac{1}{K_c^{10}}\right) \tag{30}$$

or alternately,

$$T_F = \frac{1}{A'\sigma^2\pi\nu}\left(\frac{1}{K_i^{10}} - \frac{1}{K_c^{10}}\right) \tag{31}$$

where $N_F = \nu T_F$, the number of cycles to failure where the cyclic load is applied at a frequency ν. Fracture safe design requires the detection of the initial flaw, a_i, before it grows this rapidly under stable conditions to critical size within the life expectancy of the structure.

If carbon fiber-epoxy resin composites are to be used, therefore, under compressive load cycling, it would be advisable to periodically remove the

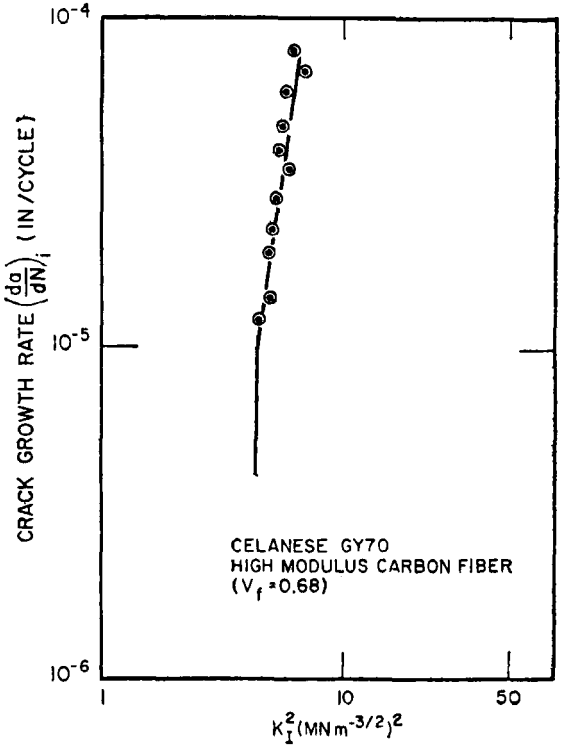

FIGURE 15 Initial crack growth rate in a carbon fiber-epoxy resin composite as a function of stress intensity factor (K) during compressive load cycling.

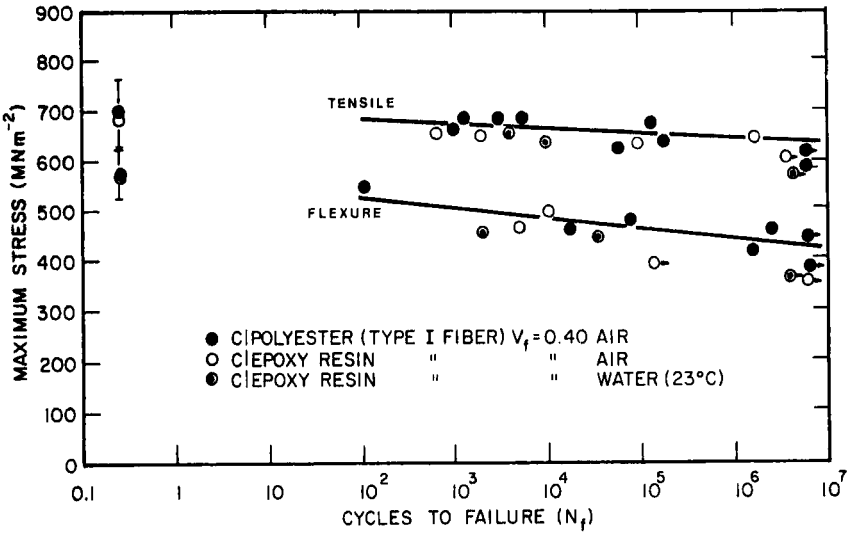

FIGURE 16 Fatigue of carbon fiber-epoxy resin composites during tensile load cycling.[19]

component from service and apply it to tensile load cycling. As reported by Beaumont and Harris,[19] tensile fatigue induces longitudinal cracks to form at the tip of transverse cracks thereby removing the uncracked portion of the material from the cracked region. Under tensile load cycling the fatigue strength of the composite is notch insensitive and determined essentially by the properties of the carbon fiber. Unstable or catastrophic failure of the composite in tensile fatigue will only occur within 10^7 cycles providing the maximum stress is greater than about 80 percent of the unnotched fracture strength (Figure 16). The apparent inferior fatigue properties of the carbon fiber composite when subjected to flexural cycling compared to tensile fatigue shown in Figure 17, reflects the poor compressive fatigue resistance pointed out by Berg and Salama. Crack initiation occurs early in the fatigue life of the material at the compressive face and extends rapidly to the neutral plane of the specimen. If these materials are to be designed so as to resist compressive crack propagation, then the resistance of the composite to failure parallel to fibers must be maximized thereby preventing sites of fiber microbuckling from linking up.[18] Attention must therefore be given to improving the fracture toughness of the resin matrix and fiber-matrix interphase region.

Since the natural points of weakness in these composites are the matrix and fiber-matrix interface, it is logical to directly attack these areas in fatigue studies in an attempt to understand better their influence on dynamic crack

propagation. In order to evaluate more quantitatively the influence of matrix and bond strength on cyclic behavior, Beaumont and Harris[19] investigated the torsional fatigue characteristics at constant strain of unidirectional carbon fiber composites. Firsty, they defined a critical threshold failure level in terms of a decrease in shear modulus, G, of the composite as the material degraded. Two levels of failure were considered:

(1) where the initial shear modulus, G, had fallen by 10 percent, i.e., where $G' = 0.9\,G$, and (2) where $G' = 0.75\,G$.

Figure 18 shows the surface treated carbon fiber composite exhibited a greater fatigue life compared to the lower bond strength material by an order of magnitude when cycled in the middle stress range, although both behaved very similar at low and high stress levels. The effect of various environments on dynamic crack growth is shown in Figure 19. Exposing the composite to steam has encouraged the propagation of cracks more easily than those evaluated in air or oil. The correlation between relaxation

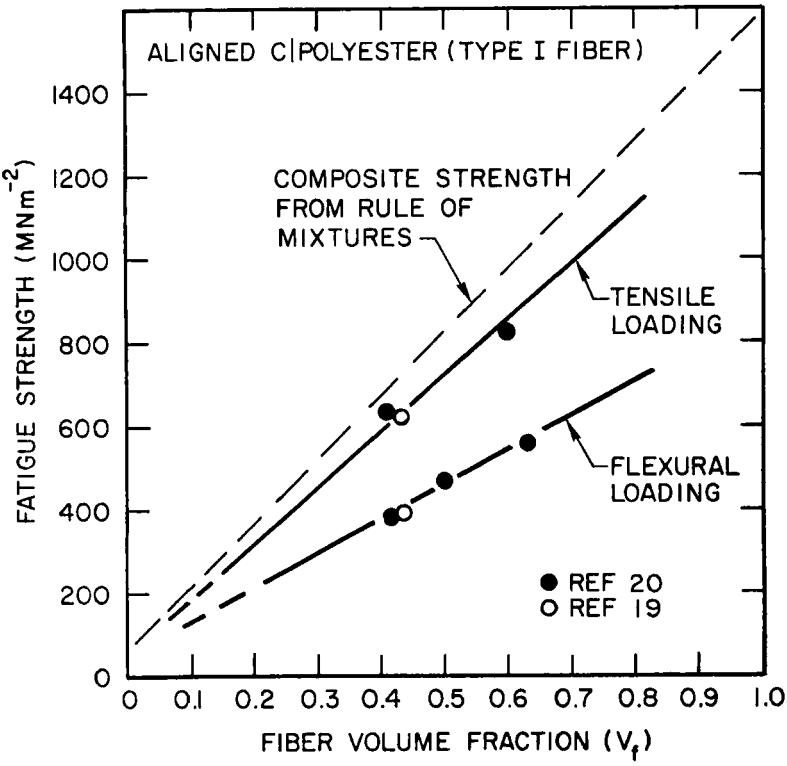

FIGURE 17 Tensile and flexural fatigue strength of carbon fiber-epoxy resin composites as a function of fiber volume fraction.

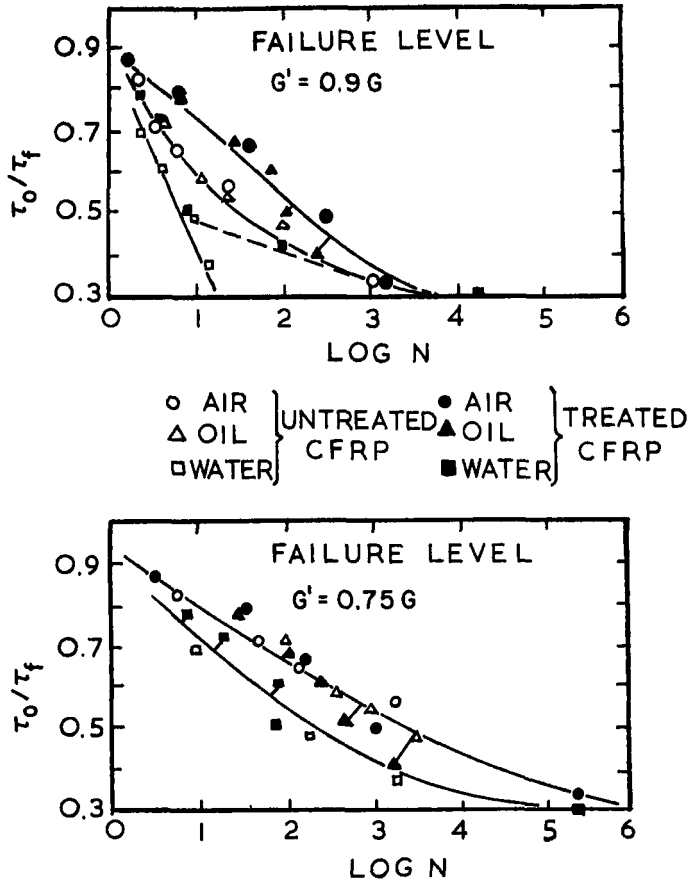

FIGURE 18 Number of reversals required for initial shear modulus, G, normalized to G/G' to fall to some arbitrarily defined level of failure.[19] (τ_0 and τ_f are the initial and ultimate shear stress of the fibrous composite.)

of modulus (or shear stress) and cracking in the matrix and at the fiber-resin interface is shown in Figure 20. There are two separate curves running parallel to one another representing results obtained from samples tested in air, oil and water. Extrapolation of these curves back to the first cycle suggests that the effect of soaking the material in a steam environment prior to testing in water introduces effectively, a degree of cracking prior to cyclic loading, as a result of decohesion between fiber and matrix. The fracture toughness of both the surface untreated and surface treated fiber composites in the longitudinal direction after exposure to moisture is reduced due to the increased brittleness of the resin matrix.[6] This resulted in the reduction

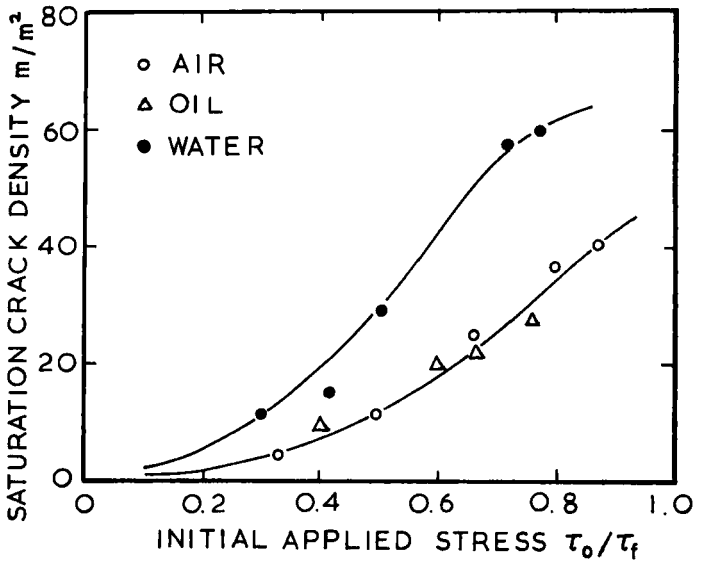

FIGURE 19 Saturation crack density as a function of the normalized initial shear modulus G/G', for surface treated carbon fiber-epoxy resin composites tested in air, oil and water. The saturation level is taken to be the density of cracks at 10^6 cycles.[19]

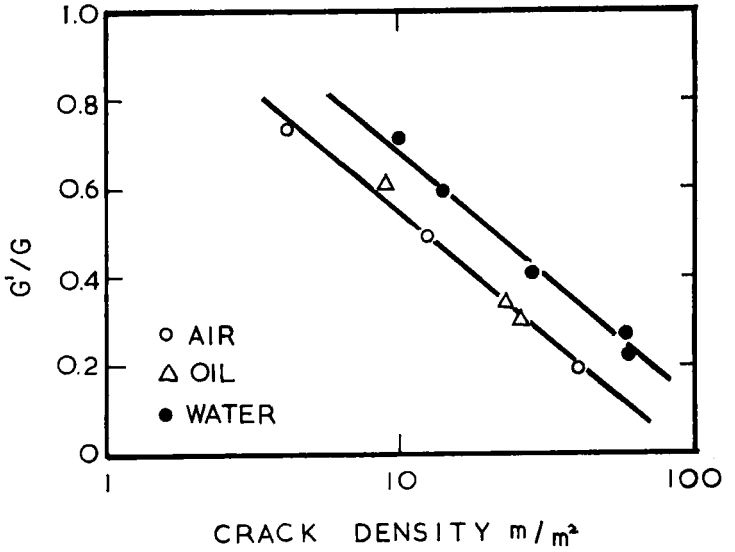

FIGURE 20 Correlation between the relaxation of modulus during torsional fatigue cycling of surface treated carbon fiber-epoxy resin composites and the density of cracks for tests in air, oil and water ($V_f = 0.40$).

in fatigue life of the high bond strength composite by order of magnitude after exposure to moisture, and a corresponding increase in crack density by a factor of 2. This suggests that slow crack propagation in carbon fiber-epoxy resin composites during torsion cycling is controlled by the toughness of the matrix. The properties of the fiber-resin interface, the effect of fiber surface treatment, and the effect of environment appear to be important only insofar as they affect locally the progress of crack propagation in the matrix.[19]

VIII FINAL REMARKS

The aims of this paper have been to demonstrate the usefulness and limitations of linear elastic fracture mechanics analysis for predicting the fracture stress and fatigue life of a range of brittle fiber-reinforced thermosetting resins. Two groups of materials have been identified where fracture occurs when, (1) the applied load exceeds the average failure load of the fibers (notch insensitive weakly-bonded composites) and (2) when the stress concentration at a crack tip exceeds the fracture stress of the next unbroken fiber (notch sensitive, strongly-bonded composites). In both instances, the fracture stress is proportional to the fiber volume fraction.

The important material parameters affecting the initiation and propagation of cracks in these kinds of fibrous composites have been reviewed. Two groups of behavior exist, where (1) fracture toughness is related to the capability of the fiber to store elastic strain energy, $G(\sigma_{f(u)}, E_f)$ and (2) where a large amount of irreversible "plastic" work is done at the crack tip, in the form of fiber pull-out energy, $G_p(\tau_i', l_c)$.

The high specific fracture stress of fibrous composites may offer many design advantages but a much greater awareness of the stress and environmental conditions which can result in crack nucleation, crack propagation and fracture are necessary.

Acknowledgment

The author would like to acknowledge the financial support of the National Science Foundation, Contract No. NSF GH 34421.

References

1. G. R., Irwin, *Handbuch der Physik* **6** (Springer-Verlag, Berlin, 1958), pp. 551–590.
2. G. C., Sih, P. C. Paris and G. R. Irwin, *Int'l J. Fract. Mechanics* **1**, 189 (1965).
3. S. W., Tsai, Monsanto/Washington Univ. ONR/ARPA Assoc. HPC-68-61, (1968).
4. Fracture Toughness Testing and Its Implications, *ASTM STP* 381 (ASTM, Philadelphia 1964).
5. H. G. Tattersall and G. Tappin, *J. Mat. Sci.* **1**, 296 (1966).

6. Peter W. R. Beaumont, Ph.D. Thesis, Univ. of Sussex, England (1971).
7. Peter W. R. Beaumont and D. C. Phillips, *J. Composite Materials* **6**, 32, Composite (1972).
8. Peter W. R. Beaumont and D. C. Phillips, *J. Mat. Sci.* **7**, 682–686 (1972).
9. Peter W. R. Beaumont and A. S. Tetelman, AIME Conference, 4th Spring Meeting, Boston, May 8–11 (1972).
10. See for example A. Kelly and G. T. Davies, *Met. Reviews* **10**, 1 (1965).
11. J. Fitz-Randolph, *et al.*, *J. Mat. Sci.* **7**, 289–294 (1972).
12. J. O. Outwater and M. C. Murphy, 24th Annual Tech. Conf., Reinforced Plastics/ Composites Div., SPI (1969).
13. A. H. Cottrell, *Proc. Roy. Soc. Series A* **282**, 2 (1964).
14. Peter W. R. Beaumont and B. Harris, *J. Mat. Sci.* **7**, 1265 (1972).
15. L. J., Broutman, *ASTM STP* 452 (ASTM, Philadelphia, 1968).
16. C. Ellis and B. Harris, Institute of Physics meeting on Failure Modes in Fiber Composites, University of Surrey, Guildford, England, July (1972).
17. D. Harris, A. S. Tetelman and F. Darwish, *ASTM STP* 505 (ASTM, Philadelphia, 1972).
18. C. A. Berg and M. Salama, MIT Report, Dept. of Mechanical Engineering (1972).
19. Peter W. R. Beaumont and B. Harris, 1st International Conf. on Carbon Fibers, Institute of Plastics, London, February (1971).
20. M. J. Owens and S. Morris (1970); 25th Annual Tech. Conf. Reinforced Plastics/ Composites Division of SPI, Section 8-E.